Emerging Science Innovation, vol. 4, 2024, pp. 01-16

A New Aspect in Analysis and Improvement of Standalone Solar-Driven Absorption Refrigeration Systems

Osman Wageiallah Mohammed [1,*] Fathelrahman Ahmed Elmahi [2]

[1] Faculty of Engineering, Red Sea University, Port Sudan, Sudan

[2] Department of Mechanical Engineering, Nile Valley University, Atbara, Sudan

Received 09 June 2024; received in revised form 28 August 2024; accepted 29 August 2024

DOI: https://doi.org/10.46604/emsi.2024.13833

Abstract

Solar-driven absorption refrigeration systems (ARSs) are subjected to work under off-design conditions due to the driving temperature variation. In this study, a model of NH_3/H_2O ARS with 100-kW cooling capacity has been developed. Energetic and exergetic coefficients of performance (COP, ECOP), besides cooling production (Q_{eva}), have been investigated at off-design conditions. The analysis indicates a reduction in the effectiveness of the generator and solution heat exchanger (SHX) under such conditions. A new method to improve the off-design system's performance by modifying the generator and SHX heat capacities is suggested. Results revealed that an increase in heat capacities of the generator and SHX (UA_{gen}, UA_{SHX}) effectively improves the system's performance. Raising the values of UA_{gen} and UA_{SHX} by 20% maintains the system's COP, ECOP, and Q_{eva} near their designed values under a wider range of driving temperatures (100 °C to 92 °C). Moreover, this adjustment helps decrease the system's cut-in/off temperature.

Keywords: solar refrigeration, ammonia-water system, off-design conditions, absorption refrigeration, solar energy

1. Introduction

International Energy Agency reported that current energy supply and usage are unsustainable from economic, environmental, and social perspectives [1]. International Institute of Refrigeration stated that about 15% of the world's electricity is consumed in air conditioning and refrigeration [2]. It is observed that around 80% of the total world electricity is generated from fossil fuels which contribute significantly to CO_2 emissions [3]. This is expected to raise the world's summer temperature to 3 – 4 °C by the end of this century as reported by Mishra et al. [4]. Global warming and high living standards will also raise the demand for refrigeration and air-conditioning, which in turn will enforce a substantial increase in energy consumption [5]. On the other hand, several places in the world are enjoying abundant solar energy. This ample renewable and clean power source makes the idea of solar cooling an appropriate alternative to traditional systems. Therefore it is envisaged as being feasible for the societies residing in remote areas and the communities that are suffering from insufficient electricity supplies [6-9].

Absorption systems have been regarded as one of the best options in the field of solar cooling [10, 11] and can be driven thermally by solar collectors. In addition, adsorption systems have some important advantages, including the usage of environment-friendly refrigerants, long service life, and high reliability [12]. Absorption refrigeration systems (ARSs) work with the same principle as the conventional vapor-compression systems; however, the mechanical compressor is changed by

* Corresponding author. E-mail addresses: alwagee@live.com, alwagee@rsu.edu.sd

English language proofreader: Hao-Lun Chang

a thermal compressor. ARS is typically composed of a generator (gen), condenser (con), evaporator (Eva), absorber (abs), and solution pump.

Energy is added to this system in the form of heat through the generator to produce refrigerant that condenses in a condenser and then gives a cooling effect in the evaporator. However, its high initial cost seems to be the main hindrance to its widespread adoption [13]. Therefore, more research is still needed to develop these systems into an economically viable and efficient substitute.In absorption refrigeration systems, ammonia-water (NH_3/H_2O) is commonly used as working fluid. Here ammonia is the refrigerant, and water is the absorbent [14].

This pair has many advantages like low freezing point, zero ozone depletion, zero global warming potentials, and the system can be air-cooled [2]. However, the toxicity and flammability (at high concentrations in air) of ammonia are factors that have restricted its use to areas having decent ventilation. Three key parameters usually are used to measure and compare the system's performance under different working conditions. The first parameter is the coefficient of performance (COP), which represents a ratio between the net refrigerating effect (cooling power), and the total energy supplied to the system. The second one is the exergetic coefficient of performance (ECOP) which can be defined as the total exergy output to total exergy input.

While obtained cooling power in the evaporator (Qeva) is used as the third parameter for evaluating system performance.In solar-driven absorption refrigeration systems, hot water produced by solar collectors is used to drive the system. The synchronicity between the production of hot water and cooling loads features its applicability. Principally typical absorption refrigeration system consists of four heat exchangers, i.e. generator, condenser, evaporator, and absorber. Usually, two heat exchangers are added to improve the system’s performance, namely solution heat exchanger (SHX) and refrigerant heat exchanger (RHX) [2]. In these six devices, heat transfer takes place at three temperature levels, generation, condensation absorption, and evaporation. Hence, once condensation-absorption and evaporation temperatures are determined, there is a specific generation temperature (T_{gen}) with which the maximum coefficient of performance (COP) is achieved. Several simulations and experimental studies have been carried out concerning single-effect ammonia-water solar absorption refrigeration [15, 16].

Most of the conducted studies concentrated on assessing the system performance at different design points and maximizing the system COP. J. Aman et al. [6] performed a parametric study for a 10 kW solar-driven ammonia-water absorption system, which is air-cooled. Analysis of this research showed that maximum exergy loss (63%) occurs in the absorber. Recently Mendiburu et al. [17] studied the system performance under the weather in Porto Alegre, Brazil. The system's cooling power ranged from 18.9 kW to 11.3 kW depending on weather conditions. Worth mentioning that no such work has been reported that can provide performance improvement of AARS at off-design conditions.

Thermoeconomic optimization and thermodynamic design of the system have necessitated the use of heat capacity (UA) of heat exchangers in designing and sizing the system’s components. In this regard, Gebreslassie et al. [18] performed UA detailed thermoeconomic optimization of AARS. Bangotra and Mohjan [19] carried out a UA analysis of the system’s components. A similar study in this context was done by Lavanya and Murthy [20]. All the above-mentioned studies undertook the analysis of UA and the system’s performance at the design point.

No specific research could be cited in the literature for the optimum area of heat exchangers when the considered system is working in a situation other than the design point.Commercially, few single-effect NH_3/H_2O solar absorption chillers are commercially available nowadays. As presented by Jakob et al. [21] SolarNext has introduced a 10 kW unit for air-conditioning. The chiller gives its maximum output with a hot water temperature of 95 ^oC. However, its output drops sharply to about 3.8 kW only as the hot water temperature decreases to 80 ^oC. Another unit based on single-effect AARS, with 150 kW cooling capacity using hot water in the range of 98 ^oC – 88 ^oC, has been produced by Colibri company. The main characteristic of solar

energy is its variation in intensity, which is affected by different hours of the day and specific seasons of the year [22, 23]. This fact restricts the standalone solar-driven ARS to work under off-design conditions for most of the day. Working at off-design conditions significantly influences the system's capacity. In the early morning, the hot water used to drive the system returns from the solar collector with low temperatures due to less solar irradiance.

With the progress of daylight hours, solar radiation over the collector increases, consequently, the hot water goes to the absorption system at a higher temperature. In the late afternoon, solar irradiance decreases and so does the hot water temperature. This situation compels the generator to work at off-design temperature most of the day [24]. A generator temperature lower than its designed value influences the potential of the whole system conspicuously. Therefore, it would be beneficial to conduct a study that enhances the capability of the system while working in off-design conditions. Specific objectives of the present work are:

- To develop an off-design model for a single-effect ammonia-water absorption refrigeration system (AARS).
- To investigate the performance of the system at off-design conditions.
- To suggest a modification in the design of the absorption refrigeration system so that it's functioning at off-design conditions is to be advanced.

2. System description

The absorption system under consideration is a single-effect AARS as shown in Fig.1 It can be divided into two sub-systems, which are the solar sub-system and cooling sub-system. The former comprises solar collectors (a set of evacuated tube solar collectors), a hot-water tank, and two pumps. The cooling sub-system mainly contains the absorption cycle. Hot water from the storage tank is used to heat the generator and vaporize NH_3 from a strong solution. The rectifier decreases the water content in ammonia vapor by cooling it, and then the condensed water returns to the generator (stream 2).

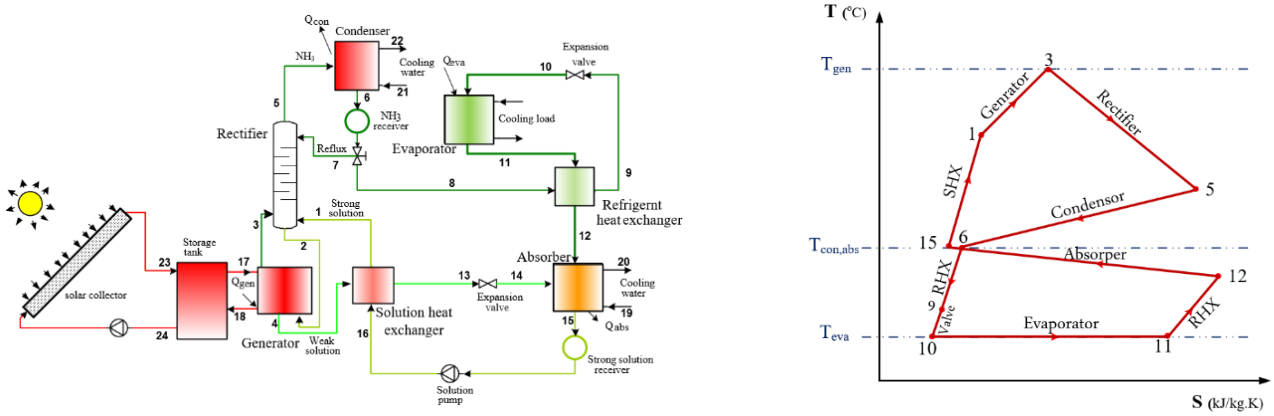

(a) Single-effect NH_3/H_2O solar absorption refrigeration system (b) Real T-S diagram of NH_3/H_2O absorption cooling cycle

Fig. 1 Flow sheet and T-S diagram of the ammonia/water absorption system

The objective of utilizing SHX is to heat the strong solution before entering the generator and to precool the weak solution ahead of the absorber. In this system, pumps and valves are controlled by an on/off controller based on temperature differences [25]. The Pressure and temperature ranges (used in the present study) for the system's key components are stated in Table 1.

Table 1 Values of pressure and temperature range for the system's key components

Component	Temperature (°C)	Pressure (bar)
Generator	78 - 120	12.23 - 11.65
Condenser	30	11.65
Evaporator	- 4	3.68
Absorber	30	3.68 - 3.42

Merely NH_3 with high concentration enters the condenser at state (5) where it is cooled and condensed to form refrigerant which is collected in the receiver (state 6). Afterward, a small fraction of the collected condensate returns to the rectifier to form reflux. The remaining liquid refrigerant (stream 8) passes through RHX where it is sub-cooled by evaporated refrigerant leaving the evaporator (11). Later, sub-cooled refrigerant at state (9) passes through the main expansion valve (10) to reach the evaporator where it is evaporated at a low temperature to produce a cooling effect. Refrigerant vapor (12) enters the absorber to be absorbed by a weak solution.

3. Mathematical model

A simulation model is developed using Cycle-Tempo software to analyze the system's performance. This software simulates the performance of the system based on mass, energy, and exergy balances. It also includes Off-design performance. The program enables the user to assemble the system components graphically, input the necessary data, and solve the set of equations formed by mass, species, and energy balances with a robust algorithm. The calculated results can be presented in a graphical or tabular form. The analysis is executed under the following assumptions:

(1) Steady state condition.
(2) Considering that the system components are thermally insulated, heat losses to the environment are neglected.
(3) Saturation state at rectifier exit (at the pressure of condenser).
(4) Saturation states at the condenser and absorber outlets as the refrigerant and strong solution, respectively, leave without subcooling.
(5) Rectifier possesses a constant efficiency.
(6) Complete condensation occurs through the condenser (only reject the latent heat of condensation).
(7) Expansion valves are adiabatic.
(8) Weak solution leaves the generator with the highest temperature.
(9) Refrigerant goes to the evaporator as a mixture of NH_3/H_2O and not as pure ammonia. So, the effects of water content are considered.

In addition to the mentioned assumptions, values of some parameters were taken from the literature [26, 27]. So, at base condition; effectiveness of solution and refrigerant heat exchangers (ε_{SHX} and ε_{RHX}) = 0.8 and pump efficiency (η_{pump}) = 0.65. Reflux ratio = 0.2 to produce refrigerant with concentration 0.998. The temperature of hot water decreases by 10 ^oC as it crosses the generator. Pressure losses are taken as $\Delta P/P = 0.05$ between the generator and condenser and as $\Delta P/P = 0.075$ between the evaporator and absorber. In both cases, P is the pressure at the pipe exit. Thanks to the software which allows users to set the pressure difference through each pipe or component.

The model is developed based on energy, mass, and species conservation equations. These basics are applied to all system units. Each unit is regarded as a control volume (Fig. 1) with in/out streams, work, and heat transfer exchanges [14].

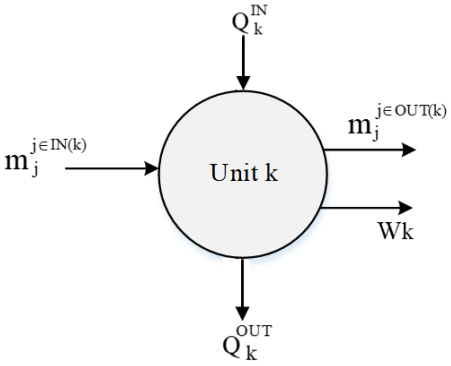

Fig. 2 Generic unit of absorption system

The subsets IN and OUT represent incoming and outgoing process streams respectively. Subsequently, the system modeling can be accomplished using the following equations. For a process unit k, the total mass balance can be written as:

$$\sum_{j\in IN(k)} m_j - \sum_{j\in OUT(k)} m_j = 0 \qquad \forall k \tag{1}$$

The component mass balance can be written as:

$$\sum_{j\in IN(k)} m_j x_{i,j} - \sum_{j\in OUT(k)} m_j x_{i,j} = 0 \qquad \forall k, i \tag{2}$$

Eq. (1) confirms that the total mass that enters unit *k* must be equal to the mass that leaves *k*. Eq. (2) intends that the total incoming mass of component *i* to unit *k* is equivalent to the total outgoing mass of component *i* from unit *k*. Where m_j represents the mass flux of stream *j* and $x_{i,j}$ denotes the mass fraction of component *i* in stream *j*.

Energy balance:

$$\sum_{j\in IN(k)} m_j h_j - \sum_{j\in OUT(k)} m_j h_j + Q_k^{IN} - Q_k^{OUT} - W_k = 0 \quad \forall k \tag{3}$$

Eq. (3) indicates the system energy balance under the assumption without any heat losses. It should be noted that the values of work and heat terms in this equation are zero in some system components as expressed by Eqs. (4) – (6).

$$Q_k^{IN} = 0 \quad \text{when k} = \begin{cases} \text{Condenser (con)} \\ \text{Refrigerant heat exchanger (RHX)} \\ \text{Absorper (abs)} \\ \text{Solution heat exchanger (SHX)} \\ \text{Expansion valves (RV, SV)} \end{cases} \tag{4}$$

$$Q_k^{OUT} = 0 \quad \text{when k} = \begin{cases} \text{Generator (gen)} \\ \text{Evaporator (eva)} \\ \text{Refrigerant heat exchanger (RHX)} \\ \text{Solution heat exchanger (SHX)} \\ \text{Pump (P)} \\ \text{Expansion valves (RV, SV)} \end{cases} \tag{5}$$

$$W_k = 0 \qquad \forall k \neq pump \tag{6}$$

Thermodynamic properties of the NH_3/H_2O pair are obtained by Ziegler and Trepp equations. The logarithmic mean temperature difference ΔT_k^{lm} is used to model all heat exchangers. So:

$$Q_k = U_k A_k \Delta T_k^{lm} \qquad \forall k \tag{7}$$

In Eq. (7), U_k is the overall heat transfer coefficient and A_k is the heat transfer area, and ΔT_k^{lm} can be defined as:

$$\Delta T_k^{lm} = \frac{\Delta T_k^h - \Delta T_k^c}{\ln \frac{\Delta T_k^h}{\Delta T_k^c}} \qquad \forall k \tag{8}$$

Where: ΔT_k^h is the temperature difference on the hot side and ΔT_k^c is the temperature difference on the cold side. The effectiveness of SHX and RHX are given by Eqs. (9) and (10) respectively.

$$\varepsilon_{SHX} = \frac{T_4 - T_{13}}{T_4 - T_{16}} \tag{9}$$

$$\varepsilon_{RHX} = \frac{T_8 - T_9}{T_8 - T_{11}} \tag{10}$$

The reflux ratio is defined as:

$$\text{Reflux} = \frac{m_7}{m_6} = \frac{m_7}{m_7 + m_8} \tag{11}$$

The circulation ratio (CR) is given as:

$$CR = \frac{m_1}{m_8} \tag{12}$$

Energetic and exergetic coefficients of performance (COP and ECOP) are determined via Eqs. (13) and (14):

$$COP = \frac{Q_{eva}}{Q_{gen} + W_{Pump}} \tag{13}$$

$$ECOP = -\frac{Q_{eva}\left(1 - T_o / T_{eva}\right)}{Q_{gen}\left(1 - T_o / T_{gen}\right) + W_{Pump}} \tag{14}$$

Where the reference temperature T_o is taken as 25 ºC.

4. Model validation

The results obtained by the software (temperatures, pressures, flow rates, and thermal loads) were calibrated with the experimental values. The comparison between several key values computed by the model, and those published in the cited reference is presented in Table 2.As portrayed, the results of the developed model are closer to that in the mentioned reference.The maximum absolute percentage error for the values given by cycle-tempo software is less than 7.5%, and it is below 4% for more than 90% of the obtained results. From these results can concluded that Cycle-Tempo software can be considered as a usable tool for the simulation of absorption cooling systems.

Table 2 Results of model validation

Stream No.	Temperature (ºC)			Pressure (bar)		Mass flow (kg/s)			Thermal loads (kW)			
	In [18]	model	Error %	In [18]	model	In [18]	model	Error %	Symbol	In [18]	model	Error %
1	91.9	93	-1.18	18.2	18.2	0.053	0.055	-3.64	Q_{eva}	5.0	5.0	0.00
4	104	104.3	-0.29	18.2	18.2	0.049	0.051	-3.92	Q_{gen}	8.96	8.66	-3.35
5	94	93.7	0.32	18.2	18.2	0.005	0.005	0.00	Q_{con}	5.94	5.68	-4.38
6	46.7	46.8	-0.21	18.2	18.2	0.005	0.005	0.00	Q_{abs}	8.11	7.97	-1.73
9	14.3	14.8	-3.38	18.2	18.2	0.005	0.005	0.00	Q_{SHX}	11.42	11.71	2.54
10	7.3	7.3	0.00	5.5	5.5	0.005	0.005	0.00	Q_{RHX}	0.74	0.70	-5.41
11	12.3	12.3	0.00	5.5	5.5	0.005	0.005	0.00	COP	0.55	0.56	1.82
12	31.3	33.8	-7.40	5.5	5.5	0.005	0.005	0.00				
13	54.6	54.5	0.18	18.2	18.2	0.049	0.051	-3.92				
14	54.8	54.6	0.37	5.5	5.5	0.049	0.051	-3.92				
15	46.9	46.9	0.00	5.5	5.5	0.053	0.055	-3.64				
16	47.1	47.3	-1.18	18.2	18.2	0.053	0.055	-3.64				

The system was configured on the Cycle-Tempo scheme window according to the developed model as displayed in Fig. 3. Experimental data reported by Mendes and Pereira for the ammonia-water absorption chiller at the Technical University of Lisbon is used to validate the developed model [18]. Data in the cited reference concern an ammonia-water absorption system for which 5 kW of cooling is required. These experimental resulted values are used as input data for the developed model as depicted in Fig. 3.

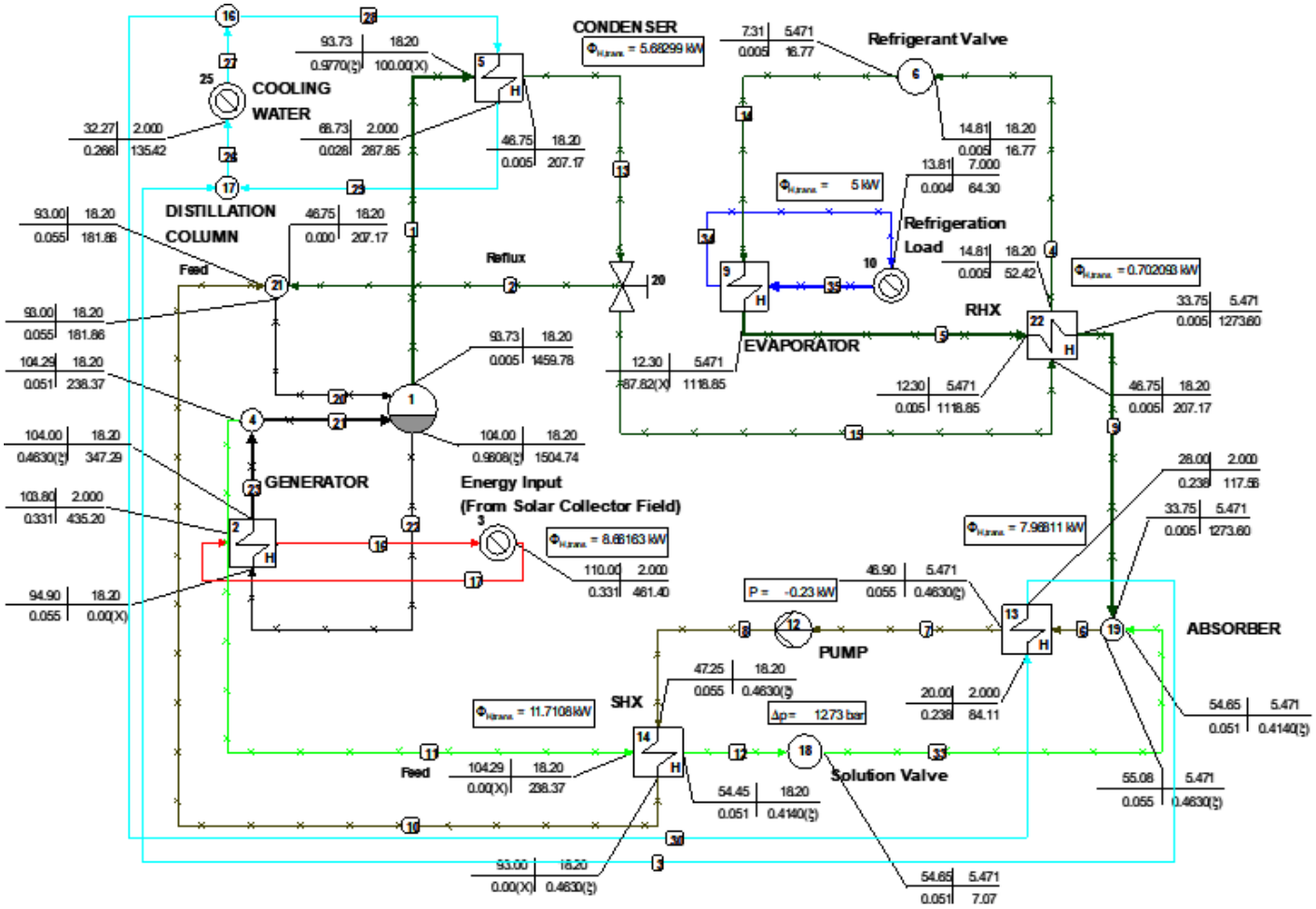

Fig. 3 Single-effect NH_3/H_2O absorption refrigeration system on Cycle-Tempo window

5. Simulation Procedure

In the present work, the system simulation has been accomplished in three main stages. Some parameters remained constant throughout the simulation process at their base values. So, $T_{con} = T_{abs} = 30$ °C, $T_{eva} = -4$ °C with 2 °C temperature glide between entrance and exit of the evaporator. At all design points the system cooling capacity is 100 kW. In the first stage of simulation, the system performance (COP and ECOP), flow rates (CR), and components' UA were investigated at different design points by varying T_{gen} from 78 °C to 120 °C.

Since the system is optimized to give its maximum performance at each T_{gen}, hence every condition represents a different design point (flow rates, component sizes, outputs, UA for each component) for the system at the given T_{gen}. A parametric study has led to choices for the design point that is given by $T_{gen} = 90$ °C as the base design condition for the system.In the second stage, the system with a specified design point has been examined at off-design conditions.

This was executed by running the simulation using values of components' heat capacity at the design point (UA_d) and designed flow rates as input for off-design calculation in the software while decreasing the temperature of hot water to emulate the real condition in solar-driven systems.The third stage of simulation deals with the improvement of the system's performance working under off-design conditions due to the decreasing of T_{gen}. Lower T_{gen} than its designed value impacts the functioning of the whole system.

The authors suggested three scenarios to address this problem: (i) increasing the UA of the SHX, (ii) increasing the UA of the generator and (iii) increasing the UA of both SHX and generator. In each of the three cases, UA has been raised gradually. And then, quantifying the effects of changing the UA of the specified components by calculating and comparing the resulting values of COP, ECOP, and CR in every case.

6. Results and analysis

By running the simulation model, the performance of the system in the above-mentioned cases has been ascertained. Based on different working situations and components' sizes, the COP, ECOP, produced cooling power (Q_{eva}), and other important parameters were calculated. Results are presented graphically in the coming subsections.

6.1. System design points at different T_{gen}

In the present study system design point is considered at $T_{con} = T_{abs} = 30$ °C, hot water and generator temperatures are 100 °C and 90 °C respectively, and cooling capacity is 100 kW. The refrigerant temperature was adjusted to – 4 °C and – 2 °C at the evaporator entrance and exit.

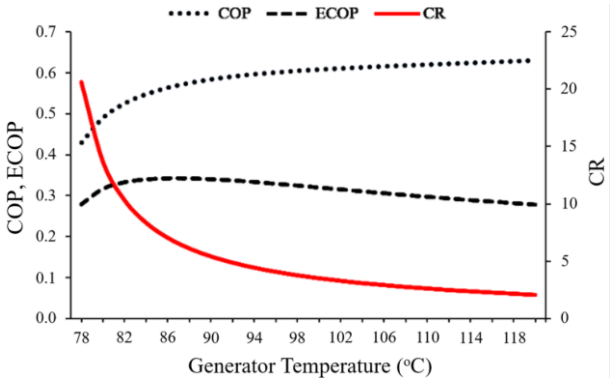

Fig. 4 Effect of T_{gen} on COP, ECOP, and CR at different design points

Results of the thermodynamic analysis for the system at base condition are depicted in Table 3. Numbers refer to points in Fig. 1. In solar-driven ARSs, the temperature of the heating source is one of the most influential parameters in system design. Fig. 4 displays the COP, ECOP, and CR for the system at different design values of T_{gen}.

Table 3 Results of system analysis at the base design condition

Point No.	Temperature (°C)	Pressure (bar)	Flow (kg/s)	NH_3 Conc. (By mass)	Enthalpy (kJ/kg)	Entropy (kJ/kg. K)
1	70.9	12.23	0.539	0.4824	78.01	0.8377
2	72.3	11.65	0.550	0.4824	84.23	0.8558
3	90.0	11.65	0.550	0.4824	392.63	1.7274
4	90.0	11.65	0.459	0.3869	174.94	1.1005
5	49.0	11.65	0.100	0.9980	1344.42	4.4639
6	30.0	11.65	0.100	0.9980	140.34	0.5023
7	30.0	11.65	0.020	0.9980	140.34	0.5023
8	30.0	11.65	0.080	0.9980	140.34	0.5023
9	4.4	11.65	0.080	0.9980	19.22	0.0850
10	-4.0	3.68	0.080	0.9980	-19.79	-0.0531
11	-2.0	3.68	0.080	0.9980	1232.18	4.5959
12	22.0	3.68	0.080	0.9980	1321.51	4.9137
13	42.14	11.65	0.459	0.3869	-44.92	0.4514
14	42.27	3.68	0.459	0.3869	-44.92	0.4542
15	30.0	3.42	0.539	0.4824	-110.76	0.2566
16	30.18	12.23	0.539	0.4824	-109.27	0.2583
Q_{gen} = 169.7 kW	Q_{con} = 120.2 kW	Q_{eva} = 100 kW	Q_{RHX} = 7.14 kW	Q_{abs} = 144.7 kW	Q_{SHX} = 101 kW	W_P = 1.34 kW
CR = 5.39	COP = 0.5846	ECOP = 0.3397				

As described for the specified system, initially as T_{gen} increases, the design values of both COP and ECOP increase while the CR decreases. Fig. 4 shows that when T_{gen} varied from 78 °C to 120 °C, values of COP changed from 0.43 to 0.63. At the same time (temperature range), ECOP ranges from 0.28 to 0.34 at T_{gen} of 90 °C, and it falls to 0.28 later. While the CR is

decreasing continuously from 20.6 to become only 2.04 at maximum T_{gen}. This can be explained as follows: for the system with higher design T_{gen}, more refrigerant is produced in the generator, for which a less strong solution flow rate is required.The ECOP passes through its highest rate at T_{gen} of 90 ºC, then declines steadily. This behavior can be attributed to an increase in the working solution temperature in the generator and absorber at higher T_{gen}, which leads to more exergy destruction in both components. These results are consistent with those found in the literature [6, 24, 27].

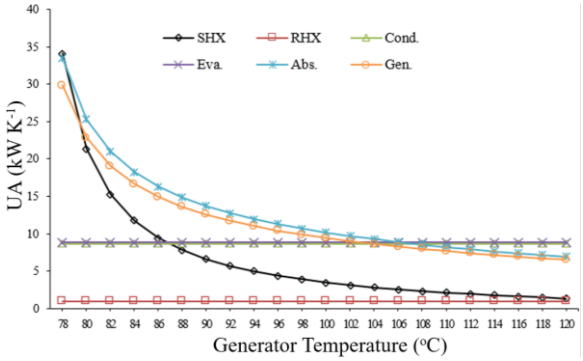

Fig. 5 Components' UA_d at different design points

Fig. 5 elucidates the basic design values of heat capacity (UAd) for six main components at different design Tgen. Moreover, Fig. 5 indicates that the UAd of SHX, generator, and absorber increase obviously as the value of Tgen decreases. In other words, systems designed to work with lower heating-source temperatures need a larger generator, absorber, and SHX. This is attributed to the increase of solution flow rate through three components at lower Tgen to attain the required cooling capacity. These observed trends indicate that the design of this system depends primarily on the temperature of the heating source, and shows that the system's performance is greatly affected by Tgen. The heat transfer capacity, mass flow rate, and terminal temperature differences for the system's components at the base design point are given in Table 4.

Table 4 Design data for system components

Component	UA_d	The mass flow rate of primary fluid (kg/s)	Terminal temperature difference (ºK)	
			High	low
Generator	12.58	0.55	10	17.7
Condenser	8.68	5.7	22	8.0
Evaporator	8.86	0.08	10.3	12.3
Absorber	13.7	4.32	13.6	8.0
SHX	6.62	0.539	19.1	12
RHX	1.00	0.08	8.0	6.4

6.2. System performance at off-design condition

As mentioned previously, the system is subjected to work under off-design conditions and is time-consuming due to a drop in hot water temperature. The performance of the designed system when working at such conditions is implied in Fig. 6.

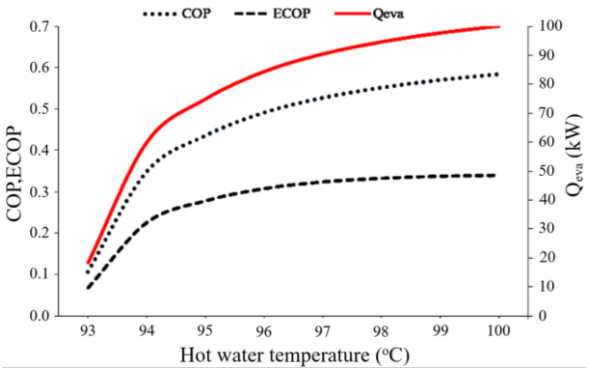

Fig. 6 System performance at off-design condition

As the heating source (hot water) temperature starts decreasing from its designed value (100 °C), the efficiency of the whole system is affected. The cooling power decreases by 40% as the hot water temperature falls from 100 °C to 94 °C. Fig. 6. also explains that this fall in temperature changes the COP dramatically (declines by 40.5%).

This happens due to two reasons, first one is the decrease of produced refrigerant (ammonia) because of lower T_{gen}. The second reason is the reduction of weak solution temperature entering the SHX which causes it to work with lower effectiveness as illustrated in Fig. 7. While the ECOP decreases gradually to the value of 0.23 at 94 °C for hot water before it drops to less than 0.08 at a hot water temperature of 93 °C. Reduction in ECOP can be attributed to more exergy losses in the generator, absorber, and SHX.

The results presented in Fig. 7 also reveal a similar behavior by the generator under off-design conditions. At the design point, the difference between hot water temperature and T_{gen} is 10 °C. However, this difference extends as the hot water temperature declines, which indicates a retraction in the generator's effectiveness. At a hot water temperature of 93 °C, the T_{gen} is only 76.4 °C. It tells that the difference is raised to 16.6 °C which is far from the designed value. In the coming subsections, the results are discussed in three different scenarios for increasing the UA of the generator and SHX to improve their working at off-design conditions.

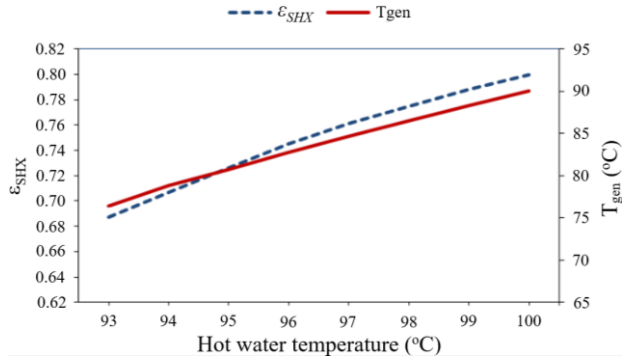

Fig. 7 Effectiveness of the SHX at off-design condition

6.3. Effect of increasing the SHX heat capacity (UA_{SHX})

At this stage, the simulation model has been running in off-design mode by using a heating source with a temperature of less than 100 °C. Five different values for SHX heat capacity (UA_{SHX}) have been employed. The designed value (UA_d) in Table 3 has been raised by 10%, 20%, 30%, 40% and 50%. For each step, the system's performance has been investigated. Fig. 8 displays the change in SHX effectiveness at different values of UA_{SHX}.

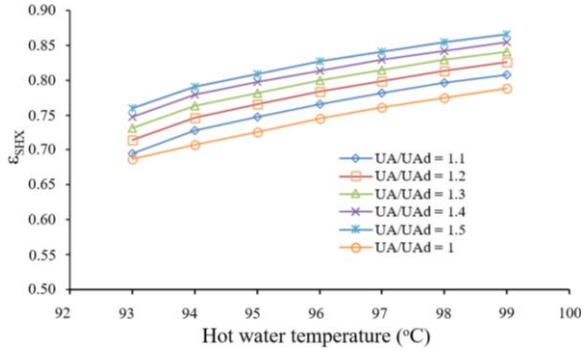

Fig. 8 Effect of increasing UA of the SHX on ε_{SHX}

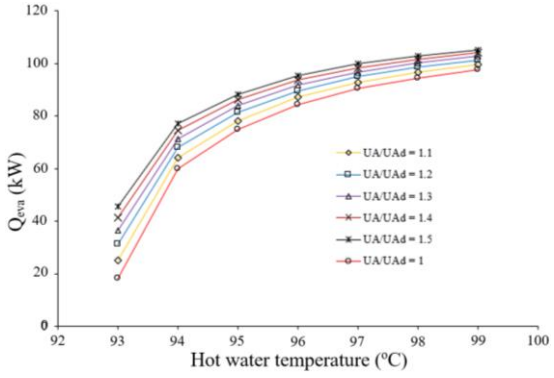

Fig. 9 Effect of increasing UA of the SHX on Q_{eva}

It further shows that ε_{SHX} is improved by increasing the component's UA. Owing to more heat transferred from the weak solution to preheating the strong solution, the subsequent improvement is established. It increases the produced refrigerant in the generator which raises the cooling power (Q_{eva}) as depicted in Fig. 9. Consequently, intensifying the produced cooling power results in a higher COP and ECOP, as illustrated by Fig.s 10 and 11.

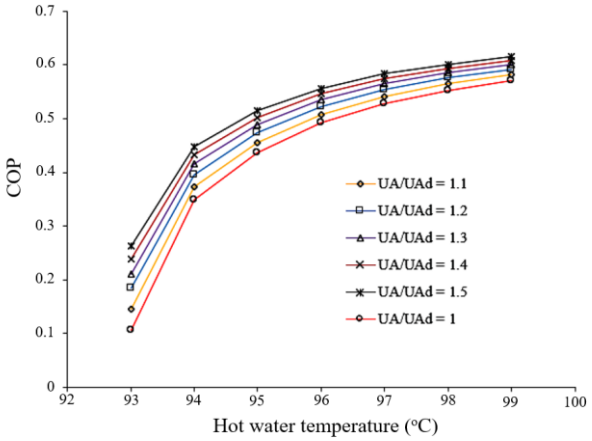

Fig. 10 Effect of increasing UA of the SHX on COP

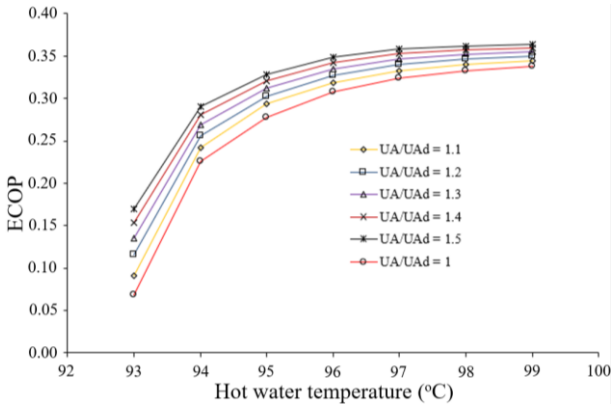

Fig. 11 Effect of increasing UA of the SHX on ECOP

Table 5 shows the values obtained for COP, ECOP, $Q_{eva,}$ and ε_{SHX} when UA_{SHX} is increased at rates of 10%, 20%, 30%, 40%, and 50% for heating source temperature 94 °C.

Table 5 Effect of increasing UA_{SHX} at a heating source temperature of 94 °C

Parameters	$UA/UA_d = 1$	$UA/UA_d = 1.1$	$UA/UA_d = 1.2$	$UA/UA_d = 1.3$	$UA/UA_d = 1.4$	$UA/UA_d = 1.5$
COP	0.35	0.37	0.40	0.42	0.43	0.45
ECOP	0.23	0.24	0.26	0.27	0.28	0.29
Q_{eva} (kW)	59.9	64.2	68.1	71.5	74.5	77.2
ε_{SHX}	0.707	0.728	0.746	0.763	0.779	0.791

6.4. Effect of increasing the generator heat capacity (UA_{gen})

The heat capacity of the generator (UA_{gen}) has been increased by 10% and 20%. The effects of this increase in the system's cooling capacity at off-design conditions are described in Fig. 12. The system's output is significantly improved. With an ascend of 20% in UA_{gen}, using a hot water temperature of 94 °C the designed Q_{eva} is reduced by 14% only. Moreover, the system's cut-in/off temperature is reduced by 2 °C since it can continue working at hot water temperature until 91 °C with acceptable output.

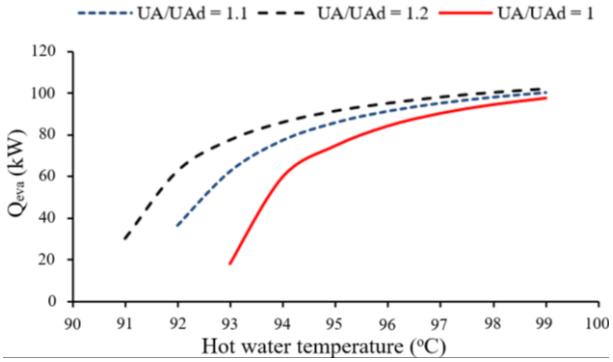

Fig. 12 Effect of increasing UA of the generator on Q_{eva}

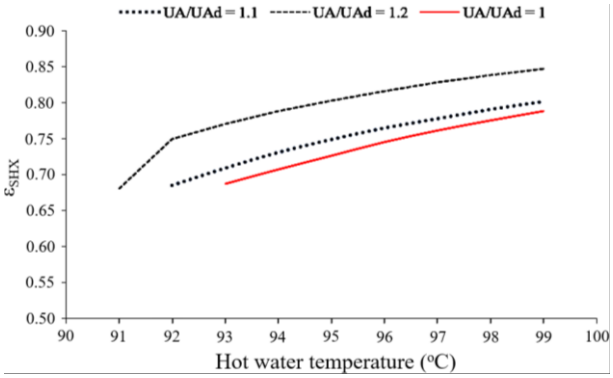

Fig. 13 Effect of increasing UA of the generator on ε_{SHX}

These improvements can be explained as follows: at high UA_{gen}, more heat is transferred from hot water to strong solution; eventually, more refrigerant is produced, and the weak solution reaches SHX with a higher temperature which effectuates its proximity to the design point (Fig. 13). In addition, the temperature difference between hot water and T_{gen} remains near designed value.

Improvement of Q_{eva} directly led to a rise in both COP and ECOP effectively, as noticed in Fig.s 14 and 15. The values of COP and ECOP are 0.1053 and 0.068 at base design with provision of 93 °C hot water temperature. A noticeable rise is witnessed in these values which arrive at 0.4523 and 0.2874 respectively with a 20% increase in UA_{gen}.

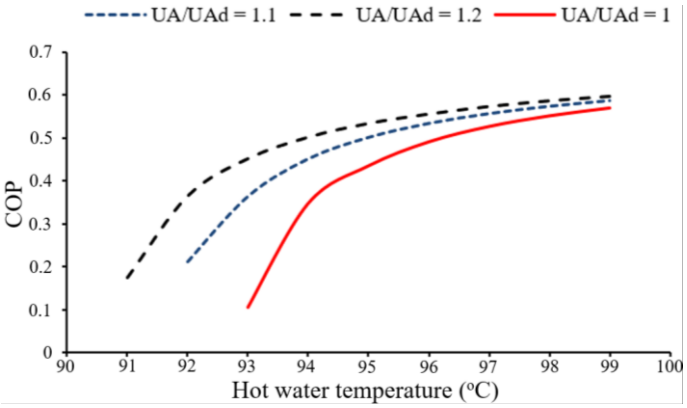

Fig. 14 Effect of increasing UA of the generator on COP

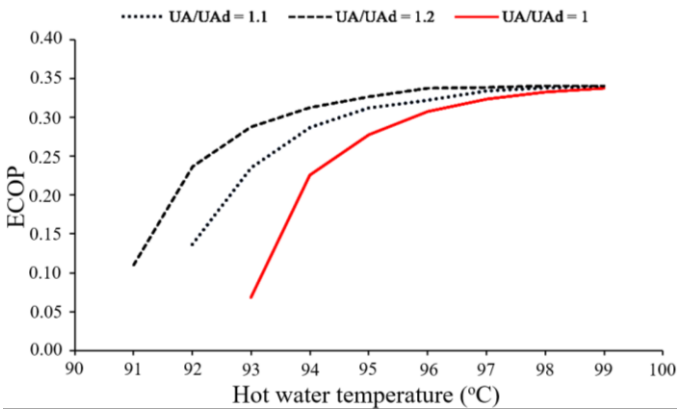

Fig. 15 Effect of increasing UA of the generator on ECOP

Specific values for improving COP, ECOP, Q_{eva}, and ε_{SHX} at each UA_{gen} increase level at a heating source temperature of 94 °C are presented in Table 6.

Table 6 Effect of increasing UA_{gen} at a heating source temperature of 94 °C

Parameters	$UA/UA_d = 1$	$UA/UA_d = 1.1$	$UA/UA_d = 1.2$
COP	0.35	0.45	0.50
ECOP	0.23	0.29	0.31
Q_{eva} (kW)	59.9	77.4	86.1
ε_{SHX}	0.707	0.731	0.788

6.5. Effect of increasing both UA_{SHX} and UA_{gen}

To present the optimal performance of the system, the advantages of increasing UA_{SHX} and UA_{gen} have been combined simultaneously. As shown in Table 4, the heat capacity of the generator is approximately twice the heat capacity of the solution heat exchanger. Therefore, increasing UA_{gen} by a significant percentage could result in a higher financial cost. In this regard, three different cases have been taken under consideration.

First case, both values are increased by only 10%. Based on the results obtained in the first case, combined with the results presented in sections 6.3 and 6.4, in the second case increasing rates are 20% for UA_{SHX} and 10% for UA_{gen}. Third case, the increase in both values is 20%.

Fig. 16 compares the system's cooling production for three situations with the output of the system without modifications. Furthermore, Fig. 16 Portrays that the system's potential can be bettered further provided increasing heat capacities are employed for both components at the same time.

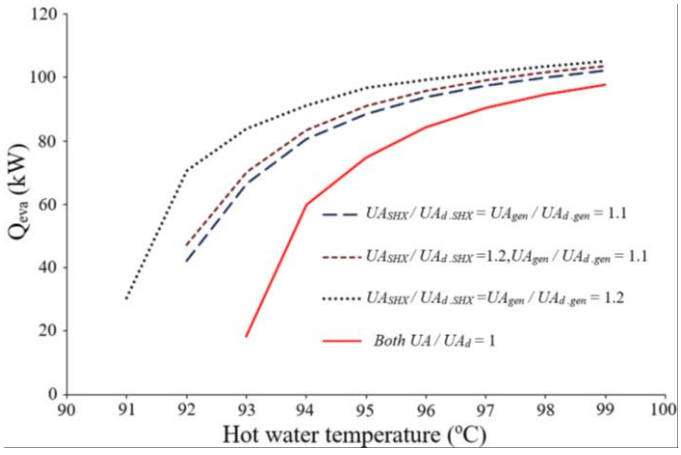

Fig. 16 Effect of increasing both UA_{SHX} and UA_{gen} on Q_{eva}

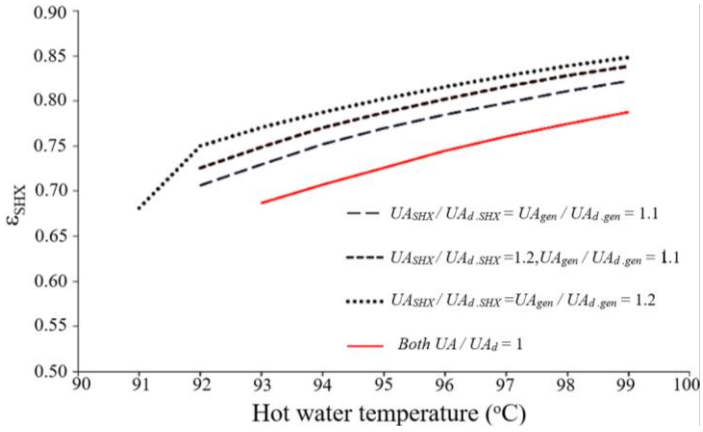

Fig. 17 Effect of increasing both UA_{SHX} and UA_{gen} on ε_{SHX}

Increasing the heat capacity of two components raises the amount of transferred heat from hot water in the generator to produce more refrigerant. The temperature uplifts of weak solution (T4 in Fig. 1) emerge to enable the SHX to function from the adjacency of its design point In addition, the increase of UA_{SHX} enhances the amount of transferred heat to a strong solution. This situation boosts the SHX to work with high effectiveness at a wider range of driving temperatures as shown by Fig. 17.

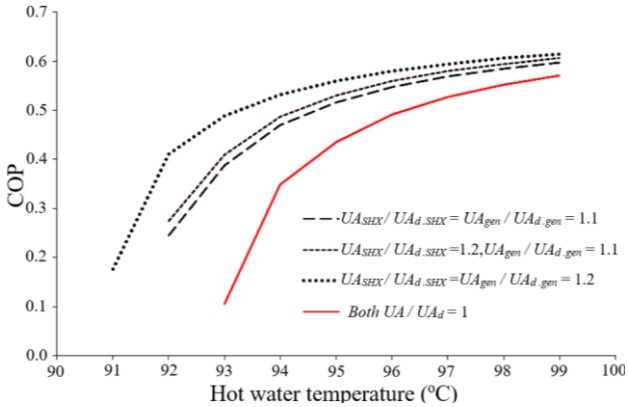

Fig. 18 Effect of increasing both UA_{SHX} and UA_{gen} on COP

In the first case, there was a significant improvement in the system's performance. Compared with the system without modifications, cooling production increased by 34.7% for a heating source temperature of 94 °C. As the temperature of the heating source decreases, the effect of increasing both UA_{gen} and UA_{SHX} becomes more clear. At a driving temperature of 93 °C (cut in/off temperature), the system with base design can produce only 18.3 kW.

This figure can be elevated to 60 kW of cooling power when the heat capacity of the two components increases by 10%. Moreover, the system will be capable to continue working till the heating temperature reaches 92 °C to produce 42.2 kW of cooling.

In case two, the heat capacity of the generator is increased by 10% while that of the solution heat exchanger is raised by 20%. Figure 16 depicts the improvement in system performance in this case. The produced cooling power has increased. However, the improvement is not high when compared with that gained by raising both UA_{gen} and UA_{SHX} by 10% only. Similar results can be delivered from Fig. 17, 18, and 19. So, increasing UA_{SHX} by 20% while keeping that for the generator at 10% will not add a significant improvement in system performance.

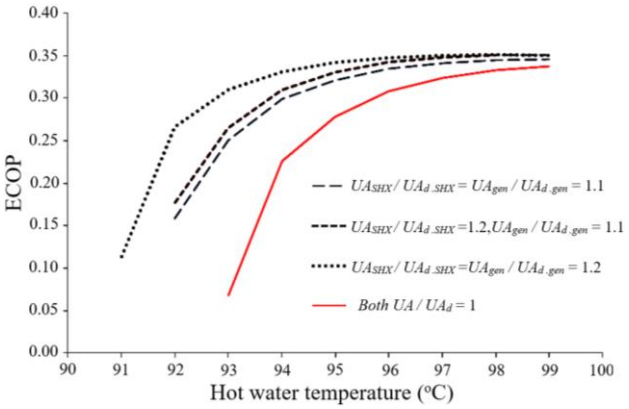

Fig. 19 Effect of increasing both UA_{SHX} and UA_{gen} on ECOP

In case three, the Q_{eva} is greater than 70% of the design capacity even if the driving temperature is reduced by 8 °C from the design value. Moreover, the system continues to produce cooling power by hot water temperature down to 91 °C. On the other hand, improvement of the system output and enhancement of heat transfer in the generator and SHX resulted in higher COP and ECOP as expressed by Fig.s 18 and 19 respectively.

Two Fig.s demonstrate that a higher performance under off-design T_{gen} is acquired with rising UA_{SHX} and UA_{gen} both by 20%. In this case, the COP attained by a hot water temperature of 93 °C is 0.4878 as compared to only 0.1053 at the base

design. Further, the ECOP is as high as 0.31 which is 350% greater than its value at the base design for the same working temperature. Table 7 summarizes the results of changes in UA_{gen} and UA_{SHX} for the three cases.

Table 7 Effect of increasing both UA_{gen} and UA_{SHX} at a heating source temperature of 94 ^{o}C

Parameters	Both UA /UA_d = 1	UA_{SHX} /$UA_{d,\ SHX}$ = 1.1	UA_{SHX} /$UA_{d,\ SHX}$ = 1.2	UA_{SHX} /$UA_{d,\ SHX}$ = 1.2
		UA_{gen} /$UA_{d,gen}$ = 1.1	UA_{gen} /$UA_{d,gen}$ = 1.1	UA_{gen} /$UA_{d,gen}$ = 1.2
COP	0.35	0.47	0.49	0.53
ECOP	0.23	0.30	0.31	0.33
Q_{eva} (kW)	59.9	80.7	83.6	91.1
ε_{SHX}	0.707	0.752	0.770	0.788

7. Conclusion and recommendations

Solar-driven absorption refrigeration systems are subjected to work at off-design conditions for many hours per day due to the nature of solar energy. The main goal of this study is to analyze and improve the performance of a single-effect ammonia-water solar absorption refrigeration system, working at off-design conditions due to a decrease in heating source temperature. To get it materialized, a steady-state model of AARS is developed to evaluate the system's performance under off-design conditions.

According to the results of the off-design performance analysis, three scenarios for the system's improvement have emerged. Based on the obtained results following findings are prescribed:

(1) The performance of stand-alone solar-driven absorption refrigeration systems considerably decreases when working at off-design heating source temperature. Therefore, substantial efforts are required to overcome this shortcoming.

(2) For the system under consideration, the generator and SHX are directly affected by decreasing of heating source temperature to less than the designed value. Therefore, improving the off-design performance of these two components can enhance the output of the whole system effectively.

(3) Increasing the UA_{gen} and UA_{SHX} by 10% over their base design values can deliver a relatively high increase in the system's off-design performance from a view of cooling production, COP, and ECOP.

(4) A further increase in UA_{SHX}, without a corresponding increase in UA_{gen}, does not bring a significant improvement in system performance when it works at off-design heating temperature.

(5) Results expose that the increase in UA_{gen} has a more positive impact on the system's performance. However, increasing both UA_{SHX} and UA_{gen} simultaneously, by the same percentage, can deliver the highest improvement in the system's off-design performance. Moreover, this can reduce the system's cut-in/off temperature. In this regard, the analysis showed that raising both UA_{gen} and UA_{SHX} by 20% can let the system produce cooling power at a rate of 91% of its base design even when the heating temperature is lower by 6 ^{o}C than its design value.

(6) Results of this study discovered that fixing the components' sizes of standalone solar-driven ARS should not be restricted to base design conditions only. Since such systems are expected to work under off-design conditions due to variations in driving temperature within day hours. The performed simulation proved that increasing the heat capacity of the generator and solution heat exchanger can improve the off-design system's performance and make it more flexible to the change in driving temperature.

To conclude, the new aspect in the analysis of NH_3/H_2O ARS, when working at off-design conditions, can be considered as a useful source to improve this system's performance under the mentioned circumstances. The study outcomes can assist

the upcoming research in this field. However, further research is required to investigate the optimal level of UA_{gen} and UA_{SHX} increase considering cost and performance trade-offs. Besides, exploring control strategies for improving the system's off-design performance is essential.

Nomenclature

Abbreviations			
ARS	Absorption refrigeration system	T	Temperature (°C)
AARS	Ammonia-water absorption refrigeration system	lm	Logarithmic mean temperature (K)
COP	Coefficient of performance	S	Entropy (kJ/kg. K)
ECOP	Exergetic coefficient of performance	Reflux	Reflux ratio
UA	Heat capacity (W/ °C)	P	Pressure (kPa)
U	Overall heat transfer coefficient (W/m^2. °C)	IN	Going in
A	Heat transfer area (m^2)	OUT	Going out
SHX	Solution heat exchanger	RV	Refrigerant valve
RHX	Refrigerant heat exchanger	SV	Solution valve
X	Mass fraction of ammonia	gen	Generator
CR	Circulation ratio	o	Reference state
m	Mass flow rate (kg/s)	d	Design point
Q	Heat transfer rate (kW)	k	Component
W	Work rate (kW)	con	Condenser
H	Specific enthalpy (kJ/kg).	eva	Evaporator
H	Hot side	abs	Absorber
c	Cold side	pump	Solution pump
Greek symbols			
ε	Effectiveness	η	Efficiency
Δ	Difference in any quantity		

Conflicts of Interest

The authors declare no conflict of interest.

References

[1] D. Vérez, E. Borri, and L. F. Cabeza, "Trends in Research on Energy Efficiency in Appliances and Correlations with Energy Policies," Energies, vol. 15, no. 9, article no. 3047, 2022.

[2] O. W. Mohammed and G. Yanling, "Comprehensive Parametric Study of a Solar Absorption Refrigeration System to Lower Its Cut In/Off Temperature," Energies, vol. 10, no.11, article no. 1746, 2017.

[3] I. Karakurt and G. Aydin, "Development of Regression Models to Forecast the CO2 Emissions from Fossil Fuels in the BRICS and MINT Countries," Energy, vol. 263, part A, article no. 125650, 2023.

[4] V. Mishra, U. Bhatia, and A. D. Tiwari, "Bias-Corrected Climate Projections for South Asia from Coupled Model Intercomparison Project-6," Scientific Data, vol. 7, article no. 338, 2020.

[5] Y. A. M. Ahmed, O. W. Mohammed, O. M. E. S. Khayal, and E. B. Elagab, "Absorption Cooling System Utlizing Diesel Engine Exhaust Heat," International Journal of Engineering Applied Sciences and Technology, vol. 7, no. 6, pp. 74-95, 2022.

[6] J. Aman, D. S. K. Ting, and P. Henshaw, "Residential Solar Air Conditioning: Energy and Exergy Analyses of an Ammonia-Water Absorption Cooling System," Applied Thermal Engineering, vol. 62, no. 2, pp. 424-432, 2014.

[7] O. W. Mohammed and G. Yanling, "Yearly Energetic and Exergetic Performance of Solar Absorption Refrigeration System in the Region of Northern Sudan," International Energy Journal, vol. 17, no. 3, pp. 141-154, 2017.

[8] M. Mohammed and T. J. Mourad, "Development of Solar Desalination Units Using Solar Concentrators or/and Internal Reflectors," International Journal of Engineering and Technology Innovation, vol. 12, no. 1, pp. 45-61, 2022.

[9] O. W. Mohammed and F. A. Elmahi, "Prediction of Global Solar Radiation across the Region of Northern Sudan," Journal of Karary University for Engineering and Science, vol. 3, no. 1, pp. 1-13, 2024.
[10] E. Bellos, I. Chatzovoulos, and C. Tzivanidis, "Yearly Investigation of a Solar-Driven Absorption Refrigeration System with Ammonia-Water Absorption Pair," Thermal Science and Engineering Progress, vol. 23, article no. 100885, 2021.
[11] G. Volpato, S. Rech, A. Lazzaretto, T. C. Roumpedakis, S. Karellas, and C. A. Frangopoulos, "Conceptual Development and Optimization of the Main Absorption Systems Configurations," Renewable Energy, vol. 182, pp. 685-701, 2022.
[12] G. Leonzio, "Solar Systems Integrated with Absorption Heat Pumps and Thermal Energy Storages: State of Art," Renewable and Sustainable Energy Reviews, vol. 70, pp. 492-505, 2017.
[13] V. Jain, A. Singhal, G. Sachdeva, and S. S. Kachhwaha, "Advanced Exergy Analysis and Risk Estimation of Novel NH3-H2O and H2O-LiBr Integrated Vapor Absorption Refrigeration System," Energy Conversion and Management, vol. 224, article no. 113348, 2020.
[14] K. E. Herold, R. Radermacher, and S. A. Klein, Absorption Chillers and Heat Pumps, 2nd ed., Florida: CRC Press, 2016.
[15] A. Aliane, S. Abboudi, C. Seladji, and B. Guendouz, "An Illustrated Review on Solar Absorption Cooling Experimental Studies," Renewable and Sustainable Energy Reviews, vol. 65, pp. 443-458, 2016.
[16] T. S. Ge, R. Z. Wang, Z. Y. Xu, Q. W. Pan, S. Du, and X. M. Chen, et al., "Solar Heating and Cooling: Present and Future Development," Renewable Energy, vol. 126, pp. 1126-1140, 2018.
[17] A. Z. Mendiburu, J. J. Roberts, L. J. Rodrigues, and S. K. Verma, "Thermodynamic Modelling for Absorption Refrigeration Cycles Powered by Solar Energy and a Case Study for Porto Alegre, Brazil," Energy, vol. 266, article no. 126457, 2023.
[18] B. H. Gebreslassie, M. Medrano, F. Mendes, and D. Boer, "Optimum Heat Exchanger Area Estimation Using Coefficients of Structural Bonds: Application to an Absorption Chiller," International Journal of Refrigeration, vol. 33, no. 3, pp. 529-537, 2010.
[19] A. Bangotra and A. Mahajan, "Design Analysis Of 3 TR Aqua Ammoniavapour Absorption Refrigeration System," International Journal of Engineering Research and Technology, vol. 1, no. 8, pp. 1-6, 2012.
[20] R. S. Lavanya and B. Murthy, "Design of Solar Water Cooler Using Aqua-Ammonia Absorption Refrigeration System," International Journal of Advanced Engineering Research and Studies, vol. 2, no. 2, pp. 20-24, 2013.
[21] U. Jakob, K. Spiegel, and W. Pink, "Development and Experimental Investigation of a Novel 10 KW Ammonia/Water Absorption Chiller," Proceedings of the 9th International IEA Heat Pump Conference, pp. 1-8, 2008.
[22] O. W. Mohammed and G. Yanling, "Estimation of Diffuse Solar Radiation in the Region of Northern Sudan," International Energy Journal, vol. 16, no. 4, pp. 163-172, 2016.
[23] J. A. Duffie, W. A. Beckman, and N. Blair, Solar Engineering of Thermal Processes, Photovoltaics and Wind, New York: John Wiley & Sons, 2020.
[24] N. I. Ibrahim, M. M. A. Khan, I. M. Mahbubul, R. Saidur, and F. A. Al-Sulaiman, "Experimental Testing of the Performance of a Solar Absorption Cooling System Assisted with Ice-Storage for an Office Space," Energy Conversion and Management, vol. 148, pp. 1399-1408, 2017.
[25] J. Fernandez-Seara and M. Vazquez, "Study and Control of the Optimal Generation Temperature in NH3-H2O Absorption Refrigeration Systems," Applied Thermal Engineering, vol. 21, no. 3, pp. 343-357, 2001.
[26] P. Colonna and S. Gabrielli, "Industrial Trigeneration Using Ammonia-Water Absorption Refrigeration Systems (AAR)," Applied Thermal Engineering, vol. 23, no. 4, pp. 381-396, 2003.
[27] F. Táboas, M. Bourouis, and M. Vallès, "Analysis of Ammonia/Water and Ammonia/Salt Mixture Absorption Cycles for Refrigeration Purposes in Fishing Ships," Applied Thermal Engineering, vol. 66, no. 1-2, pp. 603-611, 2014.